PNL-SA-10290
CONF-820833--15

PNL-SA--10290

DE83 002072

MASTER

OFF-GAS CHARACTERISTICS OF LIQUID-FED JOULE-HEATED CERAMIC MELTERS

R. W. Goles
G. J. Sevigny

June 1982

This paper is based on work sponsored by the Office of Nuclear Waste Management of the Department of Energy and performed under DOE Contract No. TDO-954 (AR-05-15-10)

To be presented at the 17th DOE Nuclear Air Cleaning Conference, August 2-5, 1982, Denver, Colorado

Pacific Northwest Laboratory
Richland, Washington 99352

DISTRIBUTION OF THIS DOCUMENT IS UNLIMITED

DISCLAIMER

OFF-GAS CHARACTERISTICS OF LIQUID-FED JOULE-HEATED CERAMIC MELTERS

R. W. Goles and G. J. Sevigny
Pacific Northwest Laboratory
Richland, Washington 99352

Abstract

The off-gas characteristics of liquid-fed joule-heated ceramic melters have been investigated as a function of melter operational condition and simulated waste feed composition. The results of these studies have established the identity and behavior patterns of gaseous emissions, the characteristics of melter-generated aerosols, the nature and magnitude of melter effluent losses and the factors affecting melter operational performance.

I. Introduction

Liquid-fed, joule-heated ceramic melters are to form the basis of the planned Defense-Waste Processing Facility (DWPF) to be constructed at the Savannah River Plant (SRP). The purpose of this facility (DWPF) is to isolate and immobilize defense-related nuclear waste as a borosilicate glass. The Pacific Northwest Laboratory (PNL) is assisting the Savannah River Laboratory (SRL) in establishing the design criteria or the DWPF by providing appropriate liquid-fed ceramic melter research and development and technology transfer.

Off-gas characterization studies have been established as part of the SRL-DWPF melter development program being conducted at PNL. The objective of these studies is to establish the off-gas properties of liquid-fed, joule-heated melters as a function of melter operational parameters and feed composition.

The scope of these studies is quite broad and covers all aspects of off-gas concern including: 1) effluent characterization, 2) emission abatement, 3) flow rate behavior, and 4) corrosion effects. This paper will discuss the results obtained from each of these areas after a brief description of the liquid-fed melter process.

II. Liquid-Fed Melter Processing System

The following is a brief description of the liquid-fed processing system which was developed at PNL in support of the SRP-DWPF. A much more detailed account of the liquid-fed melting process can be obtained from Reference 1.

Melter

Several processes for solidifying and immobilizing high-level (radioactive) liquid waste as a stable borosilicate glass have been and are currently being evaluated at PNL.(2) The process being evaluated in this study utilizes a joule-heated ceramic-lined melter which is directly fed a uniform slurry composed of glass formers and simulated liquid radioactive waste. Upon entry into the melter, the waste components of the slurry are oxidized and melted with the glass formers present in the feed to form a molten borosilicate glass. The power required to maintain this continuous glass production process is supplied by resistive ac heating of the melter glass pool. In addition to the primary source of power, auxiliary radiant heaters located in the melter plenum above the glass melt surface have also been employed to increase or "boost" feeding and glass production rates. Limited use has also been made of plasma and propane combustion torches to add supplement heating to the melter plenum. Figure 1 schematically illustrates the liquid-fed melting process.

Two different joule-heated ceramic melters were used in these developmental studies and are referred to as the Liquid-Fed Ceramic Melter (LFCM) which has a melting surface area of 1.05 m^2, and the Pilot-Scale Ceramic Melter (PSCM), which possesses a 0.73 m^2 surface area. The maximum glass production rates associated with these melters are nominally 40 kg/h-m^2 for unboosted operation, and 60 kg/h-m^2 when auxiliary plenum heaters are employed. Table I summarizes all important operational parameters associated with liquid-fed melter tests involving the LFCM and PSCM melters. These melter tests form the bases of the experimental off-gas studies which are discussed below.

TABLE I. Liquid-Fed Melter Operational Parameters

Operational	Experiment									
Parameters	PSCM-1	LFCM-4	PSCM-2	LFCM-6	PSCM-3	LFCM-7	PSCM-4	PSCM-5	PSCM-6	PSCM-7
Feed Type	Basic	Basic	Basic	Basic	Acidic	Acidic	Acidic	Acidic	Acidic	Acidic
Feed Rate, kg/h-m^2	45	90	110	100	62	130	120	135	165	170
Glass Prod. Rate, kg/h-m^2	22	41	50	45	28	57	39	46	65	42.5
Plenum, Temp., °C	400	600	400-800	600	250	500	400	520	850	850
Boosting Type	None	Elec. Lid Heat	Propane Combustion	Elec. Lid & Plasma Torch	None	Elect. Lid Heat	None	Elec. Lid Heat	Elec. Lid Heat	Elec. Lid Heat
Boosting Power, kW	—	30	35	40	—	15	—	36	55	44
Off-Gas Temp. °C	375	375	375	350	210	250	275	375	400	400
Off-Gas Cooling, gph	None	2	6	5	None	Variable	None	6	6	8
Experiment Duration, h	120	120	120	120	135	120	107	99	138	240

Melter Off-Gas System

Both melters being studied in this report share a common 0.1-m (4-in.) stainless steel off-gas system consisting of an ejector venturi, a downdraft condenser, a packed scrubbing tower and a final absolute filter, physically arranged in the order listed. In addition to these common off-gas elements, both melters are equipped with a close-coupled HEPA filter receptacle and a total (condensible and noncondensible) off-gas flowmeter. Since the purpose of the off-gas studies described here was to establish melter off-gas characteristics, the performance of the generic off-gas processing equipment present in the common melter off-gas system will not be discussed here.

Feed Composition

The liquid slurry feed used in the SRL-DWPF melter development program is a uniform mixture of simulated defense waste sludge and glass formers (frit). The composition of this slurry as equivalent oxides is detailed in Table II. The actual waste loading of the slurry is 29 wt% of the total oxides present. In addition to the major elemental constituents listed in Table II, SRL simulated waste also contains stable elemental substitutes for all volatile and semivolatile isotopes which are present in typical defense waste and which are of radiological concern. The trace elemental composition of the SRL feed slurry is presented in Table III.

Although the waste composition of the liquid feed remained essentially constant throughout the period of testing covered in this report (see Table II), the rheology of the feed was dramatically affected with the addition of formic acid to the DWPF waste stream flowsheet. Initial experiments were conducted with an alkaline (pH 11 to 12) slurry having the physical characteristics of a Bingham plastic fluid. Acidification (pH 5 to 6) of the liquid waste stream with formic acid resulted in slurries which behaved more like an ideal Newtonian fluid. The presence of formic acid in melter feed slurries not only changed the fluidic properties of the feed, but it also dramatically influenced the off-gas emission properties of the liquid-fed melter.

III. Melter Effluent Characterization

One of the major tasks involved in the DWPF off-gas studies was that of determining melter emission characteristics. The nature and extent of melter-generated effluents had to be established before off-gas system criteria could be finalized for the DWPF melters. Consequently, an off-gas sampling system was developed to provide this basic off-gas design data.

Melter Off-Gas Sampling Network

The sampling network, which was developed in support of melter emission characterization studies, is schematically illustrated in Figure 2. The components making up this network were designed to determine the composition of melter exhaust with regard to the effluents listed below.

- Gases:
  - H_2
  - N_2
  - O_2
  - CO
  - CO_2
  - SO_2
- Semivolatiles:
  - Cs
  - Sb
  - Se
  - Te
  - Mn (Tc)
  - Ru
  - Cd (Cm)
  - Sr
  - Halogens
  - Others
- Particulates

TABLE II. Simulated Waste Slurry and Glass Compositions

Waste Slurry Composition			
Alkaline Waste		Acid Waste	
Compound	Conc., g/L	Compound	Conc., g/L
Frit-131	338.0	Frit-131	341.3
Zeolite	14.7	Zeolite	9.9
Anth. Coal	3.30	$HCHO_2$	>18.0
$Fe(OH)_3$	90.9	$Fe(OH)_3$	81.2
$Al(OH)_3$	21.0	$Al(OH)_3$	34.2
MnO_2	19.5	$Mn(CHO_2)_2$	28.2
$Ni(OH)_2$	10.4	$Ni(CHO_2)_2$	8.3
$CaCO_3$	8.90	$Ca(CHO_2)_2$	16.7
SiO_2	5.84	SiO_2	15.6
NaOH	4.93	$NaCHO_2$	8.42
$NaNO_3$	2.01	$NaNO_3$	2.01
Na_2SO_4	0.73	Na_2SO_4	0.72

Typical Slurry and Glass Oxide Composition					
	Equivalent Oxide Concentration, g/L				
Oxide	TDSF Waste	(1) Frit-131	(2) Zeolite	Total	Final Glass Composition, wt%
Fe_2O_3	60.7			60.7	12.7
Al_2O_3	22.3		1.9	24.2	5.1
MnO	13.8			13.8	2.9
NiO	4.1			4.1	0.8
CaO	7.2		1.1	8.3	1.7
SiO_2	15.6	197.6	4.7	219.9	45.6
Na_2O	4.6	60.4	0.2	65.2	13.6
Na_2SO_4	0.7			0.7	0.1
B_2O_3		50.2		50.2	10.5
Li_2O		19.4		19.4	4.1
MgO		6.8		6.8	1.4
TiO_2		3.4		3.4	0.7
La_2O_3		1.7		1.7	0.4
ZrO_2		1.7		1.7	0.4
TOTAL	129.0	341.2	7.9	480.1	100.0

* Feed slurry glass content = 0.4784 kg/L.

** Value based on reaction of $MnCO_3$ and $HCHO_2$.

(1) Frit-131 Composition (-200 mesh).

Oxide	Wt.%
SiO_2	57.9
B_2O_3	14.7
Na_2O	17.7
Li_2O	5.7
MgO	2.0
TiO_2	1.0
La_2O_3	0.5
ZrO_2	0.5
	100.0

(2) Zeolite Composition (Linde Ionsiv IE-95)

Component	Wt.%
$CaAl_2Si_4O_{12}\cdot 6H_2O$	80
$Na_4Ca_{1.5}Al_3Si_8O_{24}\cdot 8H_2O$	20
	100

Assumed Oxide Forms	Wt.%
CaO	10.6
Al_2O_3	19.2
SiO_2	47.7
Na_2O	2.5
H_2O	20.0
	100.0

TABLE III. Concentration of Trace Melter Feed Additives

Trace Additives	Concentration, g/L	
	Oxides	Elemental
Cs_2O	0.25	0.24
SrO	0.098	0.083
Sb_2O_3	0.16	0.060
SeO_2	0.04	0.029
CdO	0.38	0.033
TeO_2	0.05	0.036
RuO_2	0.085	0.064

Real-time measurements of melter off-gas concentrations were initiated during the latter part of this study with the installation of five continuous gas monitors. These instruments have provided continuous compositional off-gas data with regard to H_2, O_2, CO, CO_2 and SO_2 for both the PSCM-5 and PSCM-6 experiments.

Characterization of the pathways and magnitudes of melter-generated semivolatile emissions were assessed using a differential sampling system composed of a filter, a heat-traced sampling line, a condenser and a series arrangement of three gas scrubbing units (Figure 2). The distribution of semivolatiles across the five discrete sample fractions generated by the system are analytically determined using emission spectrometry (ICP), atomic absorption (AA), ion chromatograph (IC) and x-ray fluorescence techniques. All semivolatile studies conducted have been exclusively concerned with characterizing the unquenched melter exhaust composition.

Melter-generated aerosols were characterized with regard to concentration, size and composition. Total off-gas particulate loading was most directly established, gravimetrically, by HEPA filtration of the entire melter off-gas stream (Figure 2). Particle size information is obtained from a cyclonic sampling system consisting of a series arrangement of three cyclones and a final absolute filter. The cut points of the cyclones employed are 16 μm, 6 μm and 1 μm at 0.75 acfm. The final absolute filter is designed to collect submicron fines which are able to pass through all three preceding cyclones. The elemental composition of the particulate matter collected by these sampling devices is established using ICP, AA and IC analytical techniques.

Melter Exhaust Composition

The noncondensible (20°C) gases generated by liquid-fed melters are functionally dependent upon the slurry feed composition as well as melter operating conditions. The semivolatile alkaline waste feed used during the initial stages of this study possessed very low concentrations of organic matter. Consequently, the gross melter off-gas composition was predominantly CO_2-enriched inleakage. The emission rates of the combustible gas CO during all of the alkaline feed tests were always less than 1/10 the rate associated with CO_2. Table IV summarizes the average gross compositional data associated with alkaline-fed melter exhausts. The dramatic difference existing between the PSCM-2 data and that of all other experiments listed in Table V is due to the method of boosting used in that test. During PSCM-2, a propane torch was used to add supplemental heat to the melter plenum in order to facilitate increased feeding rates. Consequently, the major source of off-gas combustion products was the boosting torch and not the melter. Figure 2 illustrates the time-correlated behavior of the gross composition of the melter exhaust during the PSCM-2 test. The relationships illustrated are consistent with the propane combustion process.

TABLE IV. Melter Noncondensible Off-Gas Composition

Experiment	Melter In-leakage, scfm	Molar %											
		CO_2			CO			O_2			N_2		
		Hi	Avg	Lo	Hi	Avg.	Lo	Hi	Avg.	Lo	Hi	Avg	Lo
PSCM-1	5 - 10	6.4	3.4	1.8	<0.01	--	--	20	14.0	7.1	89	81	73
LFCM-4	32	1.1	0.58	0.4	0.03	0.018	0.001	21	20.5	20.0	78	78	78
PSCM-2	45	8.6	4.6	0.2	3.0	0.50	0.001	21	14.0	8.0	82	80	79
LFCM-6	29	0.87	0.54	0.13	0.067	0.023	<0.001	20	20.0	18.0	80	79	78

The composition of melter-generated, noncondensible gases was dramatically affected when formic acid was added to the simulated melter feed. This compositional alteration increased the organic loading in the melter feed by approximately an order of magnitude. Consequently, melter exhaust gases were of particular interest during these acidified feed tests due to the possibility of generating H_2 and CO (water gas) in sufficient quantities to present a flammability hazard after off-gas quenching. Figure 3 illustrates the time-related behavior of gross melter exhaust gases during a 120-h melter test which employed 100 h of radiant lid heat boosting and 20 h of unboosted operations. The presence of plenum heaters during liquid feeding clearly reduces melter emission of the combustible gases H_2 and CO. With the termination of lid heating, the melter plenum cooled, reducing the oxidation rates of these gases sufficiently to allow significant quantities of each gas to escape the plenum through the off-gas system. This result is quite reproducible; however, virtual elimination of combustible gas emissions during boosting as is illustrated in Figure 3 may not always be achievable. Similarly, the concentration of combustibles leaving an unboosted melter may be significantly higher than is indicated in Figure 3 since they are slurry composition-, temperature-, feed- and in-leak rate-dependent variables. Indeed, dilution air was required during the unboosted PSCM-7 to reduce H_2 in the quenched off-gas stream to below 70% of its lower inflammability limit (~4%). A summary of all melter off-gas compositional data associated with formate feed testing are presented in Table V along with all pertinent process parameters.

TABLE V. Melter Noncondensible Off-Gas Components (Acid Waste)

Experiment	Melter Inleakage, scfm	Molar Percent								
		CO_2			CO			H_2		
		Hi	Avg	Lo	Hi	Avg	Lo	Hi	Avg	Lo
PSCM-3*	20	2.94	1.3	0.2	1.31	0.40	0.04	1.11	NA	0.17
LFCM-7	90	2.2	0.7	0.03	0.44	0.13	0.002	0.63	0.54	0.40
PSCM-4	20	4.4	2.9	0.5	0.75	0.44	0.20	1.3	NA	1.0
PSCM-5	30	6.5	2.8	2.0	0.9	0.35	0.1	1.8	0.8	7.1
PSCM-6	30	6.5	4.1	2.0	0.6	0.09	--	1.2	NA	--

* Sample stream diluted ~2.5 times.

The off-gas data presented in Figure 3 clearly illustrates that melter-generated emissions are not smooth and continuous functions even under the most controlled operational conditions. This behavior is due to the erratic, nonuniform way in which melter feed is dried, oxidized and melted during the liquid feeding process. Large excursions in melter gas generation rates usually occur when dammed up liquid feed lying atop an insulating layer of dry feed (the cold cap) abruptly flows out upon a hot glass surface. The liquid quickly flashes off this hot surface, producing a flow pulse composed of streams and volatile organic reaction products. Figure 4 illustrates the behavior of some of the more important melter-generated gases accompanying flow surging events. The frequency and magnitude of these surging events are positive indicators of melter system instabilities which are most often associated with erratic or overfeeding conditions.

The ability of melter-generated gases to accompany steam flow surges suggests that the evolution of combustible gases from the melter cold cap is quite prompt. Figure 5 portrays the time-dependent compositional behavior of the melter exhaust stream upon feed interruption or termination. With the exception of SO_2, none of the melter-generated gases increase in concentration when feeding was terminated. This fact implies that volatile decomposition and reaction products generated from the melter feed are formed soon after introduction of the feed into the melter environment. Consequently, significant accumulations of chemically-reactive organic feed components within the melter cold cap apparently do not occur under stable steady-state feeding conditions.

On the other hand, the increase in terminal SO_2 exhaust concentration (illustrated in Figure 5) suggests sulfur, as Na_2SO_4, may be accumulating within the melter as a molten salt. This was indeed found to be the case, as post-run inspection of the idling melter glass surface later proved. This stimulated speculation that accumulations of Na_2SO_4 could be responsible for changes in the melting capacity of liquid-fed melters that occur during the initial ~24 hours of liquid feeding/startup phase. Melter emission characteristics of SO_2 further support this notion, as in shown in Figure 6. During the initial startup phase, when the melter's ability to handle feed is limited, feed-rate normalized SO_2 emission rates are uncharacteristically low, indicating that accumulation of Na_2SO_4 is probably occurring. As processing continues at a fixed feeding rate, SO_2 emission rates gradually increase along with the melting capacity of the liquid-fed melter. It is known(3) that the presence of a molten Na_2SO_4 phase within a ceramic melter will increase the heat transfer rate between the molten glass and the feed, thereby boosting melting capacity. All of the above-mentioned liquid-fed melter characteristics are consistent with this fact.

Although Figure 6 suggests that SO_2 evolution is the predominant mechanism responsible for sulfur melter feed losses, this is true only for boosted experiments where plenum temperatures are greater than 700°C. Emission rates of SO_2 during unboosted runs are at least an order of magnitude lower than when boosting techniques are employed. However, total melter losses of sulfur are found to be more or less independent of boosting, indicating the presence of other volatile chemical channels of escape (SO_3). Filtered gas-scrubbing techniques have verified that significant concentrations of acidic volatile gases of sulfur and the halogens always exist in unquenched melter exhaust streams independent of any and all melter operating conditions. This subject will be further developed in discussions that follow.

Nature of Melter Feed Component Losses

In order to characterize the pathways and magnitudes of melter feed component losses, a differential sampling system composed of an aerosol filter, condenser and a series arrangement of three gas-scrubbing units was employed. The manner in which any given element is distributed across the five discrete sampling fractions of this device is indicative of the physical state or states that the effluents assumed. Typical data generated with this differential sampling system for a formate-fed melter is summarized in Table VI. The DF values listed in this table are melter decontamination factors, which are ratios of the rate at which feed components enter the melter to the rate at which they are evolved. Particulate DFs are partial DFs relating to only a single loss mechanism: that of aerosol emission. The data presented in the abridged table clearly shows that melter gas-phase losses to the off-gas system are only significant for Cl, S and B, which readily form volatile acid gases previously referred to. This is not to say that melter-induced volatilization has no influence upon melter losses of other feed component elements. On the contrary, the low DFs associated with the semivolatile elements, Cs, Te, Si, Sb, etc. clearly underscore the importance of this volatilization process. What is being said is that apart from the mechanisms responsible for producing airborne effluents, particulate transport through the off-gas system is the predominant loss mechanism associated with liquid-fed melter operation.

TABLE VI. PSCM-6 Particulate and Total Feed Component DFs

Element	Average DF Particulate	Total
Al	27000	22000
B	6800	100
Cd	9.9	9.9
Cl	21	2.9
Cs	14	14
Fe	1900	1800
La	2100	2100
Mn	1800	1800
Na	300	300
S	11	5.5
Sr	1800	1800
Te	3.0	3.0
Zr	22000	22000

Characteristics of Melter Aerosols

Having determined that most melter losses to the off-gas system are associated with aerosol emission, establishing the characteristics of these areosols was of particular engineering interest. The size distribution of melter-generated aerosols was established using a cyclonic particle-size analysis system, which was described earlier. Table VII details the manner in which melter particulate matter was distributed across the cyclonic sample fraction as a function of melter experiment. All melter tests, with the exception of PSCM-4, exhibited aerosol size distributions which were definitely bimodal in nature. This suggests that the overall aerosol distribution may be comprised of two independent components, each having its own characteristic size distribution. Gross compositional dissimilarities between the discrete cyclonic size fractions illustrated in Table VIII strongly reinforce the argument. Moreover, since the submicron size fraction detailed in this table contains only 12% of the total sample mass, but possesses essentially all the semivolatile matter of the sample, the mechanism responsible for the small diameter component of the overall distribution is probably a volatilization/condensation process that occurs within the melter plenum. The composition of the large cyclonic size fractions are very similar to that of the slurry feed as shown in Table IX. Consequently, the large component of the bimodal distributions must almost certainly be associated with a gross entrainment mechanism.

Since the major melter loss mechanism associated with the radiologically-important semivolatiles is associated with submicron aerosol emissions, the elemental makeup of this size fraction is of particular interest. Table X presents representative submicron compositional data collected during the PSCM-4 experiment. If one attempts to conduct a material balance for this submicron matter by assuming an oxide form for all elements except for a stoichiometric quantity of Na, which is associated with the Cl in the sample, one can account for 99% of the matter present. It should be noted that while the submicron sample fraction is quite rich in semivolatiles, it is essentially salt (83 wt% NaCl).

TABLE VII. Size Distribution of Melter Aerosols

	Average wt% Versus Cut Point			
Experiment	16 µm	6 µm	1 µm	<1 µm
LFCM-7	76.7	2.8	8.5	11.9
PSCM-4	--	0.9	3.6	95.6
PSCM-5	13.5	3.9	20.2	62.2
PSCM-6	46.1	0.5	12.7	40.7
PSCM-7	7.5	3.2	9.4	79.9

TABLE VIII. Elemental Distribution Across Cyclonic Sampling system

	Elemental Distribution, %			
Element	16 µm	6 µm	1 µm	<1 µm
Al	96.2	0.9	2.5	0.4
B	87.7	1.8	7.8	2.6
Ba	83.7	5.8	10.5	0
Ca	77.7	2.7	15.2	4.4
Cd	10.7	0.8	7.3	81.2
Ce	92.1	0	7.9	0
Cr	46.4	21.7	23.3	8.6
Cs	7.5	0	5.4	87.1
Cu	82.6	4.9	4.2	8.3
Fe	77.3	2.6	17.0	3.1
La	91.9	1.5	6.1	0.5
Li	83.2	1.5	5.3	10.0
Mg	91.5	1.6	5.8	1.1
Mn	89.4	6.4	3.6	0.6
Mo	77.5	5.6	9.8	7.1
Na	68.8	1.7	5.6	23.9
Nd	93.4	0	6.6	0
Sb	100.0	0	0	0
Se	56.9	1.9	11.4	29.8
Si	92.0	1.8	5.6	0.6
Sr	77.6	2.8	19.6	0
Te	5.5	0.4	3.2	90.9
Ti	91.2	1.8	6.0	1.0
Zr	91.6	1.6	5.6	1.2

TABLE IX. 16μm Cyclonic Sample Fraction Composition

Compound	Weight Percent	
	16 μm	Feed
Al_2O_3	3.4	5.1
B_2O_3	9.0	10.5
CaO	1.6	1.7
Fe_2O_3	14.4	12.7
La_2O_3	0.3	0.4
LiO_2	3.5	4.1
MgO	1.1	1.4
MnO	3.2	2.9
Na_2O	13.0	13.6
SiO_2	38.0	45.6
TiO_2	0.70	0.7
ZrO_2	0.27	0.4

TABLE X. Submicron Particulate Composition

Element	Elemental Wt%	Elemental Form	Compound Wt%	Feed Composition, %
Al	0.04	Al_2O_3	0.08	4.95
B	0.07	B_2O_3	0.24	9.86
Ca	0.14	CaO	0.20	1.66
Cd	0.55	CdO	0.63	0.006
Cs	2.1	Cs_2O	2.2	0.044
Cu	0.06	CuO	0.09	--
Fe	0.29	Fe_2O_3	0.41	13.69
K	0.36	K_2O	0.43	--
Li	1.1	Li_2O	2.4	3.98
Mg	0.02	MgO	0.03	1.29
Mn	0.08	MnO_2	0.13	3.25
Na	33.7	NaCl Na_2O	83.0 6.7	-- 13.88
Ni	0.03	NiO	0.04	0.76
Pb	0.04	PbO	0.05	--
Si	0.66	SiO_2	1.4	44.47
Te	0.56	TeO_2	0.71	0.006
Zn	0.02	ZnO	0.02	--
Cl	55.0	--	--	0.4
TOTAL			98.8	

Melter Emission Performance

Melter performance with regard to effluent emission is commonly expressed in terms of a unitless decontamination factor or DF. By definition, a melter feed component DF is the ratios of the rate at which that particular feed component enters the melter to the rate at which it is evolved from it. Consequently, melter DFs are related to the liquid-fed melter process efficiencies for converting feed components into a borosilicate glass. Table XI presents experimental feed component DFs for all pertinent DWPF melter tests conducted at PNL. The entries in this table are grouped according to feed type and each group is ordered with respect to the experimental melter employed. This ordering has significance with regard to the interpretation of the data. The initial melter tests conducted with alkaline feed were, with one exception, all boosted experiments (see Table I). Consequently, a major goal of all of these tests was to establish maximum melter feeding rates under a variety of plenum heating conditions. To complicate matters, an evolving slurry feed system being developed during this same period was often responsible for inconsistent feed delivery to the melter. As a result, stable steady-state operating conditions during these early melter scoping tests were rarely, if ever, achieved. The spread in melter emission performance data during this initial testing phase is in large part a reflection of the unequilibrated conditions that existed when this data

TABLE XI. Submicron Particulate Composition

	Alkaline-Fed Melter DFs					Acid Feed Melter DFs					
Element	PSCM-1	LFCM-4	PSCM-2	LFCM-6	Average	LFCM-7	PSCM-3	PSCM-4	PSCM-5	PSCM-6*	Average**
Al	11000	530	990	330	3200	190	6000	23000	14000	22000	16000
B	210	130	160	90	150	75	200	230	140	100	170
Ca	1840	260	610	180	720	62	1100	1900	1100	1200	1300
Cd	190	70	47	80	100	8.0	—	9.2	5.7	9.9	8.3
Cl	3.1	2.2	3	2.7	2.8	—	4	5	1.5	2.9	3.4
Cs	51	57	3	10	30	12	3.8	16	9.4	14	11
Fe	3800	260	680	230	1200	69	1600	2000	1100	1800	1600
La	—	—	—	—	—	—	—		11000	2100	6600
Li	1900	310	340	160	680	89	2600	3200	730	1300	2000
Mg	9000	350	920	260	2600	120	8200	—	3500	7800	6500
Mn	5700	420	630	330	1800	76	3300	2100	7100	1800	3600
Na	830	340	130	90	350	60	900	180	160	300	390
Nd	—	—	—	—	—	—	—			2500	2500
Ni	1500	260	—	930	900	—	9400	1400	580	1100	3100
Ru	32	26	48	13	30	16	—	—	—	—	—
S	1	1	19	11	8	—	8	16	4.5	5.5	8.5
Sb	—	1800	100	—	950	67	—	—	440	—	—
Se	—	—	—	—	—	1	—	—	130	—	—
Si	15000	420	1600	280	4300	120	3000	9200	5300	13000	7600
Sr	7400	204	640	290	2300	55	640	250	—	1800	900
Te	170	62	58	210	130	5.6	32	3.1	3.1	3.0	10
Ti	—	—	1400	170	790	120	4100	8700	7200	5900	6500
Zr	—	—	—	—	—	—	—	5000	30000	20000	18000
Total ± σ	1100	290	430	180 ±10	500	120 ±50	980	490 ±30	480 ±90	800 ±80	690

* Slightly different frit used in this test.

** LFCM-7 not used in averaging.

With the exception of the LFCM-7 test (melter capacity scoping study), all acid feed melter experiments sought to establish operational stability under a variety of running conditions. Table XII presents partial melter DFs associated with off-gas aerosol emission for the PSCM-5 and -6 experiments. The data associated with each of these tests were collected over several days of stable steady-state melter operation using three independent sampling devices. The internal agreement between results obtained in each test is, without question, indicative of the stability associated with each of these experiments. Consequently, effluent results of individual acid feed experiments are more representative of average melter behavior than were those associated with the alkaline feed.

A comparison of melter DFs achieved with alkaline and acidic waste slurries reveals that, with only a single exception, higher effective emission rates (lower DFs) were observed for the radiologically-important semivolatility when acidified melter waste is employed. The reducing power of the formic acid feed component apparently promotes volatilization in the plenum and thereby produces greater effective off-gas losses of these elements.

TABLE XII. Steady State Aerosol Emission Performance of Liquid-Fed Melters

PSCM-5 Boosted Test

Sample Type*	Feed Rate, L/h	Particulate Loading, mg/L	DF
C	51	0.55	470
S	72	0.49	460
S	79	0.44	510
C	81	0.61	440
HEPA	81	--	370
S	86	0.48	492
C	93	0.78	440
HEPA	93	--	670
ALL			480

PSCM-6 Boosted/Unboosted Test

Sample Type*	Feed Rate, L/h	Particulate Loading, mg/L	DF
S	68	0.29	820
HEPA	--	--	810
C	67	0.37	840
S	74	0.25	910
C	90	0.41	700
S	91	0.28	840
HEPA	--	--	720
S	58**	0.32	870
C	58**	0.54	660
ALL			800

* C = Cyclone; S = Differential Samples; HEPA = Absolute Filtration
** Unboosted Operation

Ruthenium is an exception to the above statement. Ever since melter experiments with a formate feed formulation began, no significant airborne Ru has been detected in melter exhaust streams, except for the very atypical LFCM-7 test. Feed and glass sample analyses, on the other hand, indicate significant Ru melter losses (DF = 2), and yet no specific sink has been conclusively identified to account for these losses. In all probability, Ru is being reduced by the formic acid to its elemental state, whereupon it is lost to the melter floor as slag. A surface plateout mechanism is a possible, but less likely, explanation for these losses, but no off-gas line plating has ever been found. A thorough examination of the melter and its plenum is planned to establish the nature of the observed Ru losses.

The effect of feed-boosting techniques upon overall melter emission performance has been studied under controlled conditions. If the previous melter stability comments are neglected, Table XI strongly suggests that melter DFs are dramatically reduced when boosting is employed. However, tests designed to illustrate this effect have failed to show any significant relationships between feeding rates and melter emission performance. Table XII presents gross aerosol DF values associated with the boosted PSCM-5 and PSCM-6 tests. Clearly, this data shows no correlation between feeding rates and DF. Moreover, the boosted PSCM-6 experiment did not utilize electric radiant lid heaters for the entire melter test, yet no significant differences in melter emission performance were observed throughout the experiment. Consequently, this data suggests that electric radiant plenum heaters can be employed to boost liquid feeding rates of the ceramic melter without significantly deteriorating melter emission performance.

The implementation of feed boosting techniques, however, are not without operational difficulties. The high exhaust stream temperatures (>600°C), resulting from the auxiliary plenum heaters, present various off-gas problems associated with the formation of fused off-gas-line deposits and accelerated material corrosion rates. A cooling spray (see Figure 1) has been successfully used to control exiting melter exhaust gas temperatures to 400°C or less. However, the spray nozzle itself acts to collect entrained feed. These feed deposits ultimately grow to form a local obstruction to melter off-gas flow. Although these deposits are soft and easily removed, the current cooling spray configuration clearly compromises melter off-gas system design.

IV. Melter Idling Test

Because of the high (~1000°C) plenum temperatures associated with idling (unfed) joule-heated ceramic melters, volatilization losses of radiologically-important glass components sustained during these periods could, potentially, overwhelmingly influence the overall melter source term. The composition of typical melter idling emission, which appears in Table XIII, verifies the importance of this loss mechanism for the semivolatiles. In order to determine the importance of this melter loss mechanism, emission rates of semivolatile elements were investigated as a function of plenum temperature and, consequently, melter surface glass viscosity. Temperature control was maintained through use of plenum water sprays, which cooled but did not disturb the surface of the melter glass pool.

TABLE XIII. Melter Idling Deposits

Elements As Oxides	Weight Percent		
	Gray Deposits	White Deposits	Feed
Al_2O_3	1.2	0.11	3.5
B_2O_3	14.2	1.6	9.9
CaO	0.22	0.46	1.2
CdO	0.02	0.02	0.01
Cr_2O_3	0.57	0.58	0.02
Cs_2O	3.7	8.3	0.06
Fe_2O_3	0.10	0.17	16.0
K_2O	0.79	0.85	*
Li_2O	1.92	2.6	4.1
MgO	<0.05	<0.05	1.4
MnO_2	0.05	0.05	3.8
Na_2O	31.0	31.0	15.5
NiO	0.25	<0.02	1.5
RuO_2	0.82	2.1	0.02
Sb_2O_3	<0.01	<0.01	0.008
SiO_2	<0.02	0.47	44.0
SrO	<0.005	<0.005	0.02
TeO_2	0.70	0.70	0.01
TiO	<0.01	<0.01	0.7
ZnO	0.02	0.02	0.008

* Used in sample preparation.

This study was immediately initiated upon completion of a 120-h liquid-fed melter test (PSCM-5). With a 44 L/h water spraying rate and the melter under automatic resistance control, the melter glass surface was cooled to the point that it formed a continuous nonconvective layer above the bulk melter glass pool (plenum 280°C). At 26.5 L/h spray rate, the surface viscosity decreased significantly. Convective mixing opened vents in the glass surface that migrated at random across the melter glass pool. However, plenum temperatures were not high enough to melt feed deposits formed upon the melter walls and lid during the preceding PSCM-5 experiment. Finally, the cooling spray was terminated and the melter was allowed to idle at a fixed current rate, which slowly brought the melter plenum up to 850°C. Samples were collected from the plenum during all phases of this study.

The results obtained from these plenum samples are graphically summarized in Figure 7, which characterizes the emission rates of the semivolatile elements under various idling conditions (temperature) employed during this test. These data indicate that emission rates of all semivolatile elements decreased as a function of time after the completion of PSCM-5 under the influence of a 42 L/h water-spraying rate. Reducing the cooling spray rate to 27 L/h caused measurable increases in both plenum temperature and semivolatile emission rates; however, an equilibrated plenum temperature was not achieved during the brief period (24 h) of reduced spraying.

Termination of the water-cooling spray caused the plenum temmperature to increase steadily to the point where plenum surface deposits, formed during PSCM-5, began to melt and "burn" away. This period was responsible for the dramatic peaking of emission rates of the semivolatile elements. The fact that all semivolatiles do not form maxima at the same point in time is most probably due to temperature, which was steadily increasing throughout the interval over which these maxima occur.

The plenum temperature during the last two sampling periods was ~850°C, and all plenum surfaces appeared clean. The emission rates occurring during these periods are, with the exception of Se and Te, significantly greater than the minimum emission rates exhibited by these elements during full 42 L/h spray cooling. However, these elevated idling emission rates are still significantly below those rates observed during moderate liquid feeding conditions. Specifically, the Cs emission rate expected from the PSCM for a liquid feeding rate of 50 L/h (1.1 kg/min) would be ~8 mg/min. This is twice the value observed during the hot melter idling conditions. Consequently, it appears that the plenum cooling approach, although capable of reducing emission rates of most semivolatiles (by a factor of ~10 for Cs), is of little practical value in reducing the overall melter off-gas radiological burden.

It should be noted that the effect of direct feeding water onto the surface of an idling melter has also been investigated as an alternative method for reducing idling emissions. On a qualitative as well as a quantitative basis, this approach was less a satisfactory means of cooling the plenum and melter glass surface than was the plenum spray approach. The water feeding technique produced a high degree of entrainment and aerosol carryover into the off-gas system. Moreover, at the water feeding rates used (45 L/h), convective mixing was actually exacerbated, although total melter surface flooding was never attempted. On the other hand, the water plenum spray initiated no observed entrainment and minimized or eliminated convective surface mixing.

V. Melter Flow Rates

The off-gas flow rate behavior of two liquid-fed melters has been examined over the past year as part of the SRL-DWPF melter development program. During this period of study, two separate feed formulations have been used and a variety of melter operational running conditions have been employed. The results of these studies have shown that both feed composition and melter feeding rates have a preponderant influence upon the stability of melter off-gas flow rate.

The effect of feed composition upon melter flow rate behavior is related to the physical ability of the feed components to form a structurally sound insulating layer (cold cap) between the incoming liquid feed and the hot glass surface. As portions of the insulating cold cap become calcined, structural collapse occurs, bringing dammed up liquid feed into contact with the extremely hot glass surface. This results in the flashing off of the water component (and volatile reaction products) of the feed, producing a flow pulse or an off-gas surge. The magnitude and extent of these surges are naturally dependent upon the amount of liquid feed present on the cold cap that is delivered to the hot glass surface. Consequently, an erratic melter exhaust flow rate is often indicative of an unstable, overfed operational condition. Exhaust flow rate patterns associated with stable and unstable melter operating conditions are illustrated in Figure 8.

The two melter feed formulations used in these studies exhibited significantly different melter off-gas properties. The alkaline waste formulation produced a noisy, erratic melter flow rate with surges as high as seven times that of the average flow. The acid feed, on the other hand, possessed a very compliant nonbridging cold cap, which reduced the frequency and magnitude of off-gas surging events. Average melter flow characteristics associated with each of these feed formulations are summarized in Table XIV. This data clearly shows the stabilizing influence of the formic acid feed component upon melter flow rate behavior.

TABLE XIV. Liquid-Fed Melter Flow Rate Behavior

Experiment	Feed	Average Flow, scfm	Maximum Surge, scfm	Average Surge Duration, min
LFCM-4	Alkaline	90	620	3
LFCM-6	Alkaline	90	465	3
PSCM-3	Acid	70	220	3
LFCM-7	Acid	240	710	3
PSCM-4	Acid	70	304	4
PSCM-5	Acid	80	230	3
PSCM-6	Acid	80	190	(?)

Due to the conservative, stable manner in which most PSCM runs were conducted, PSCM flow rate data associated with acidified feed is probably more representative of average melter behavior than are the values associated with the LFCM. The LFCM data, on the other hand, can be used in assessing the effects of heavy melter feeding conditions.

VI. Corrosion

Extensive metal corrosion has been observed in liquid-fed melter plenums and in associated melter off-gas lines and processing equipment. The nature of the corrosion observed suggests acidic chemical attack by volatile halogens and sulfur compounds. In order to identify suitably corrosive-resistant melter off-gas materials, corrosion coupons representing different groups of alloys were exposed to the plenum environment of liquid-fed melters during processing (300 to 500°C) and idling (850°C) conditions. The extent of corrosion as a function of operating conditions was established, gravimetrically, through coupon weight loss. The results of these studies, which are summarized in Table XV, indicate that the corrosion rates occurring during actual liquid feeding are much greater than those occurring during hot idling. In addition, titanium, tantalum and all alloys having high iron concentration were found to be quite unsuitable for liquid-fed melter service. The most promising alloys are those possessing low iron, high nickel or cobalt and a chromium content greater than 20%. Inconel-625 and the Haynes alloys were the most corrosive-resistant materials employed during this study.

TABLE LVIII. Corrosion Sample Results

Material	Exposure, h Idling	Exposure, h Operating	Weight Change, g/cm^2	Cor. Rate, cm/y	Observations Spalling	Observations Deposits*	Color**	Approximate Composition, Wt% Cr	Co	Fe	Ni	Mo	W
Inconel®-690	1134	214	−0.025	0.020	Light	Light	Blk-Silver	30	—	9.5	60	—	—
	198	214	−0.014	0.074	Light	None	Black						
	1256	214	−0.036	0.023	Light	Light	Multi						
	320	330	−0.011	0.015	Light	Light	Black						
Inconel®-625	1134	214	+0.015		None	Heavy	Brown	21.5	—	2.5	61	9	—
	198	214	+0.007		None	Heavy	Brn-Silver						
	1256	330	+0.013		None	Heavy	Brn-Black						
	320	330	+0.012		None	Heavy	Brn-Silver						
Inconel-617	122	116	−0.004	0.008	Med-Pits	Medium	Gr-Silver	22	12.5	1.5	52	9	—
	122	116	−0.013	0.024	Med-Pits	Medium	Gr-Silver						
Inconel-600	122	116	−0.008	-.015	Medium	Light	Multi	15.5	—	8	76	—	—
	122	116	−0.002	0.004	Medium	Light	Multi						
Haynes®-188	1134	214	+0.059			Very Light	Bl-Black	22	49	<3	10	—	15
	198	214	+0.004		Light	Light	Bl-Black						
Haynes®-25	1134	214	+0.005		Light	Light	Bl-Black	21	54	<3	10	—	15
	198	214	+0.003	0.008	Light	Light	Bl-Black						
	60	110	+0.001		None	None	Black						
RA®-330	1134	214	−0.025	0.020	Medium	None	Multi	18	—	47	35	—	—
	198	214	−0.036	0.015	Medium	None	Gr Spots						
RA®-446	1134	214	−0.18	0.145	Heavy	None	Multi	25	—	75	—	—	—
	198	214	−0.17	0.472	Heavy	None	Multi						
Titanium	122	116	−0.063	0.210	Heavy	None	Silver-Brn	—	—	—	—	—	—
Tantalum	122	116	-3.3	<3	Disappeared		—	—	—	—	—	—	—

* Feed Material sintered on coupon surface.

® Inconel is a registered trademark of Huntington Alloys.

® Haynes is a registered trademark of the Cabot Corporation, Kokomo, Indiana.

® RA is a registered trademark of Rolled Alloys, Detroit, Michigan.

** Bl - Blue
Blk - Black
Brn - Brown
Gr - Green

VII. Conclusion

The off-gas studies discussed in this report have sought to establish the effluent characteristics of liquid-fed joule-heated ceramic melters. The results of these studies have shown particulate emission to be responsible for most melter effluent losses. Moreover, a large fraction of the total particulate mass evolved from an operating melter is conveyed to the off-gas system by submicron aerosols which are almost exclusively responsible for semivolatile transport. Melter operational conditions have had little effect upon these results so long as quasi steady-state conditions are maintained. Even hot melter idling conditions do not significantly affect the overall melter source term.

Melter-generated gases have been found to be potentially flammable as well as corrosive. Hydrogen generation presents the greatest flammability hazard of the combustibles generated by liquid-fed melters. Off-gas dilution was required during a melter test to maintain H_2 concentrations below 70% of its lower flammability limit in the quench melter exhaust. The combustible gas CO has never achieved a quenched off-gas concentration greater than 1/10th of its flammability limit. Auxiliary plenum heating has been found to significantly reduce melter emission rates of both these combustible gases.

Significant concentrations of acidic volatile compounds of sulfur and the halogens exist in unquenched melter off-gas streams independent of melter operational conditions. These gases have been responsible for extensive corrosion observed in melter plenums and in associated off-gas lines and processing equipment. Alloys possessing low iron, high nickel or cobalt and high chromium content have been found to be most suitable for liquid-fed melter service.

VIII. References

(1) Buelt, J. L. and C. C. Chapman. 1978. Liquid-Fed Ceramic Melter, A General Description Report. PNL-2735, Pacific Northwest Laboratory, Richland, Washington.

(2) Bonner, W. F. 1979. The High-Level Waste Immobilization Program: An Overview. PNL-3094, Pacific Northwest Laboratory, Richland, Washington.

(3) Conroy, A. R., W. H. Manning and W. C. Brauer. 1966. "The Role of Sulfate in the Melting and Fining of Glass Batch," Glass Ind., February-March (1966).

FIGURES

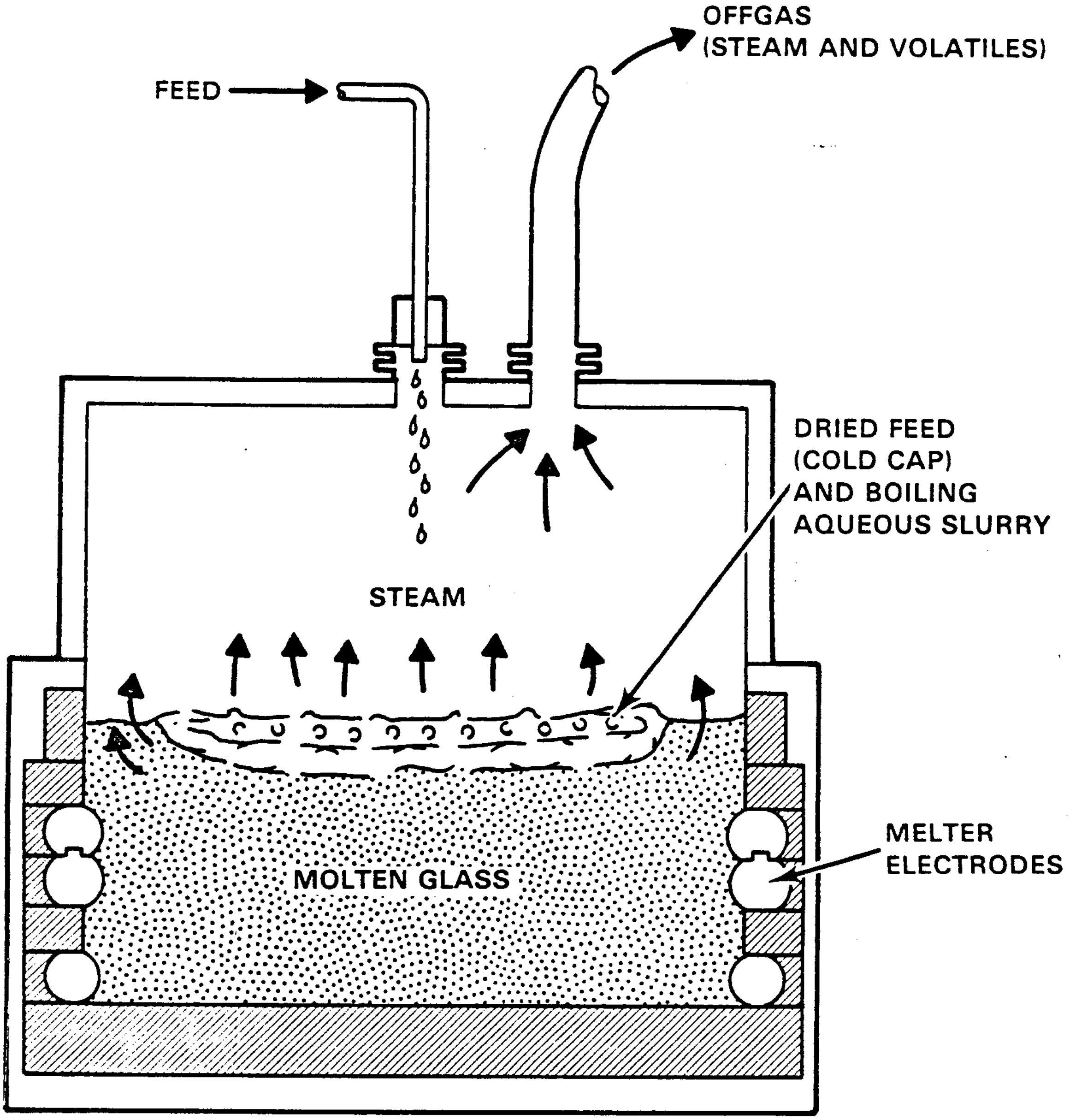

FIGURE 1. Liquid-Fed, Joule-Heated Ceramic Melter System

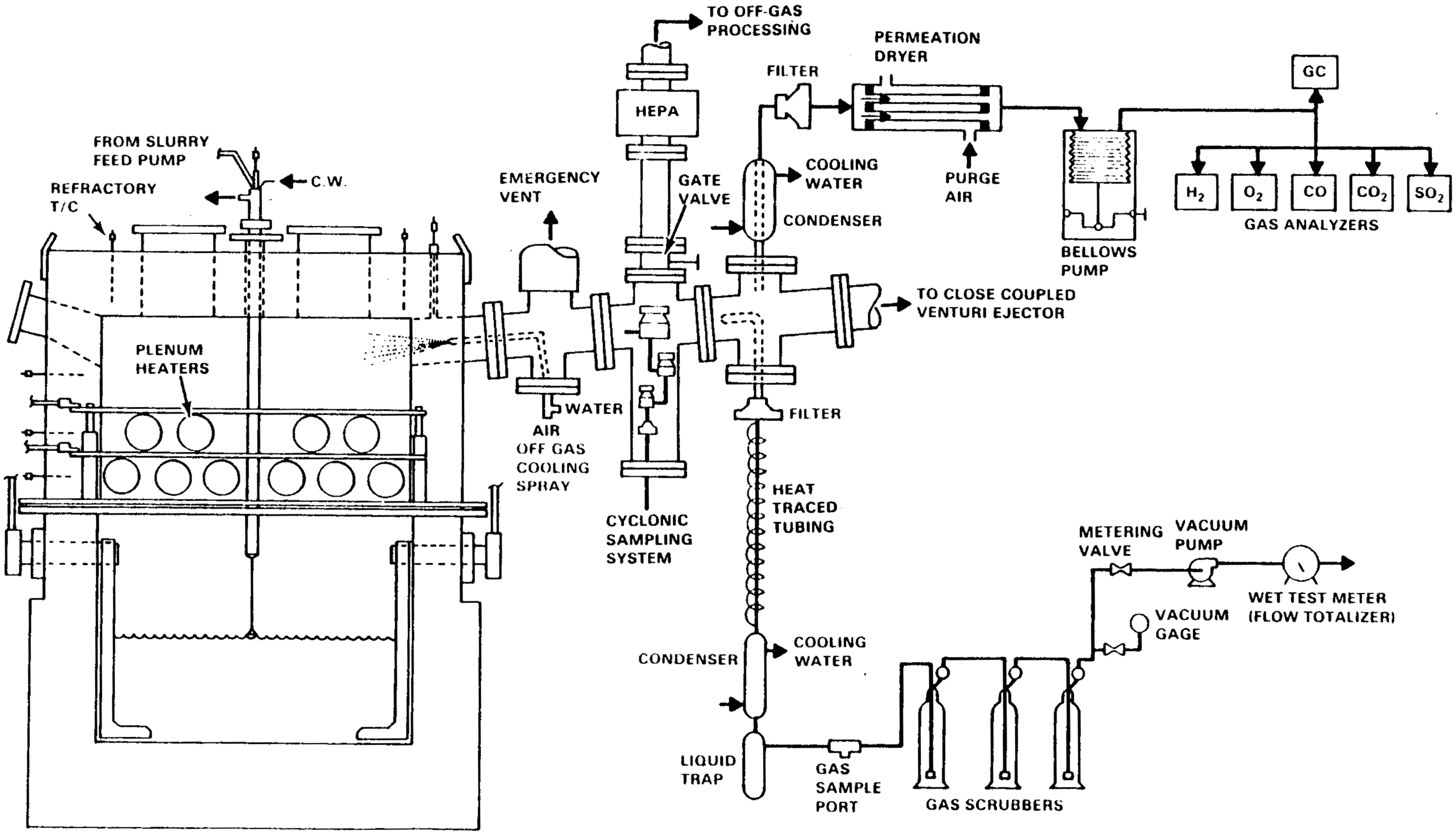

FIGURE 2. Melter Off-Gas Sampling Network

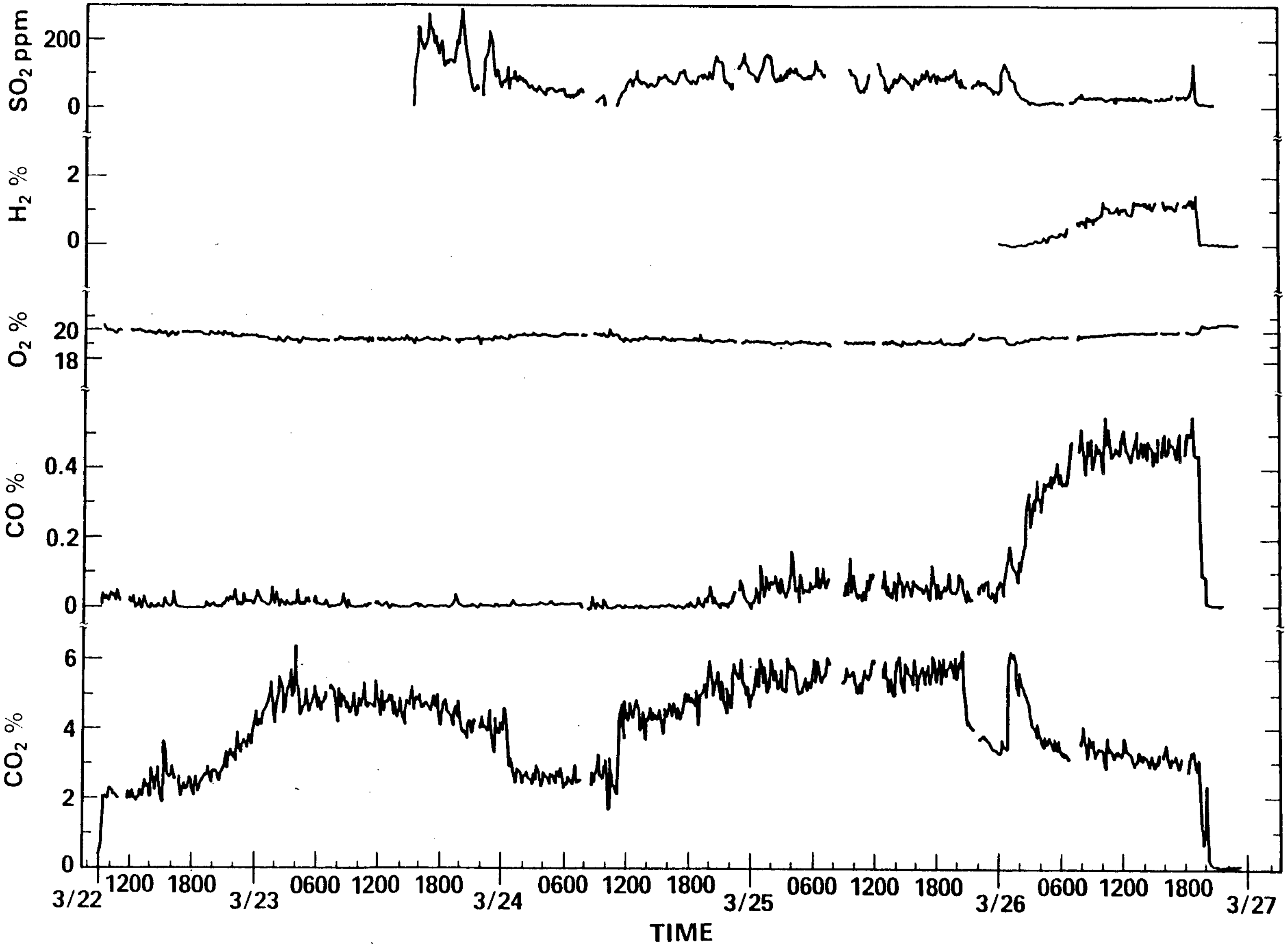

FIGURE 3. Melter Exhaust Gas Composition of a 100-h Boosted, 20-h Unboosted Test

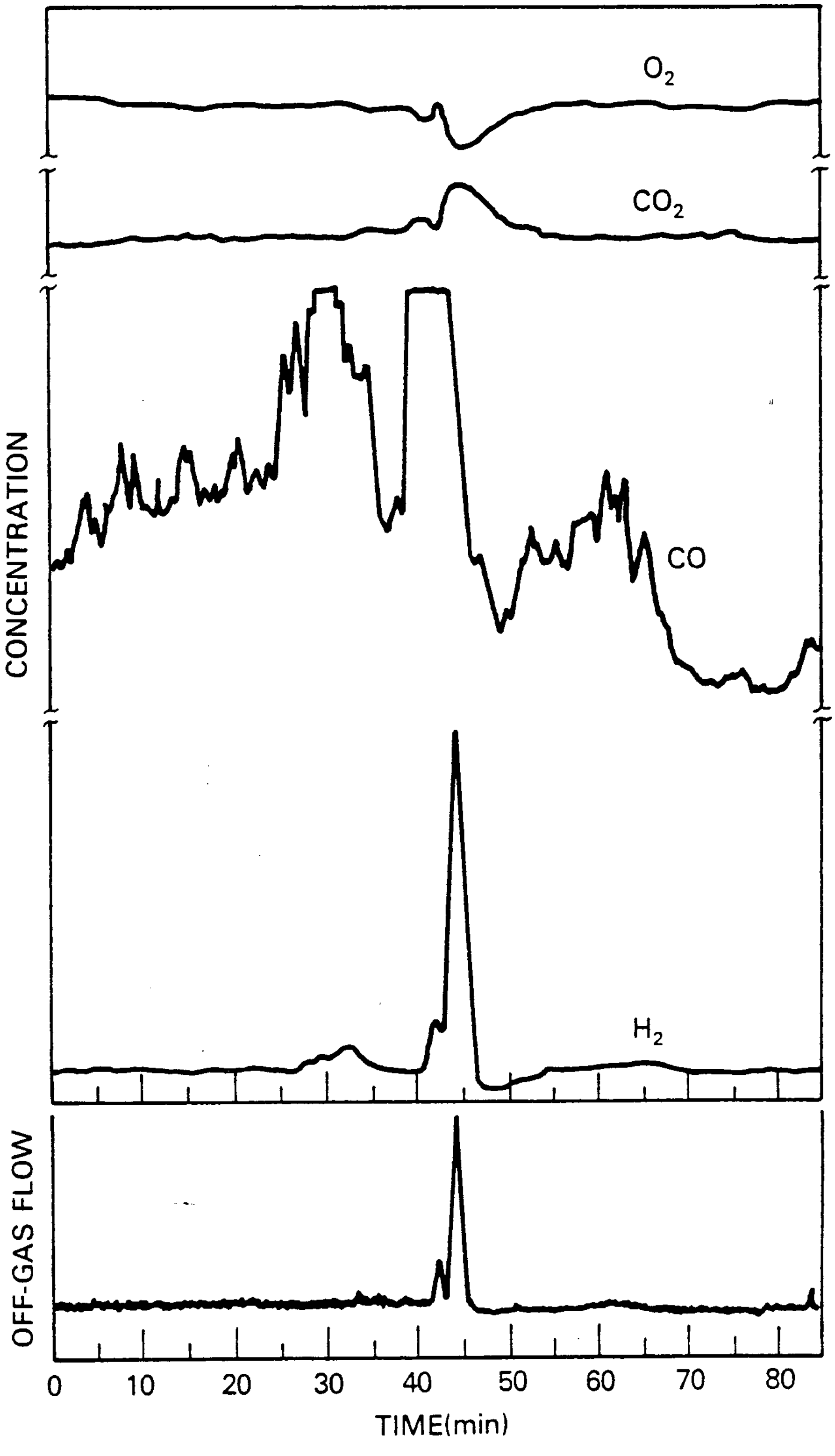

FIGURE 4. Compositional Behavior of Noncondensible Melter Exhaust Gases Accompanying a Flow Surge. Maximum Extent of the Surge Event: Flow 3X; H_2 <3.5%; CO >>0.5%; CO_2 15%; O_2 17%

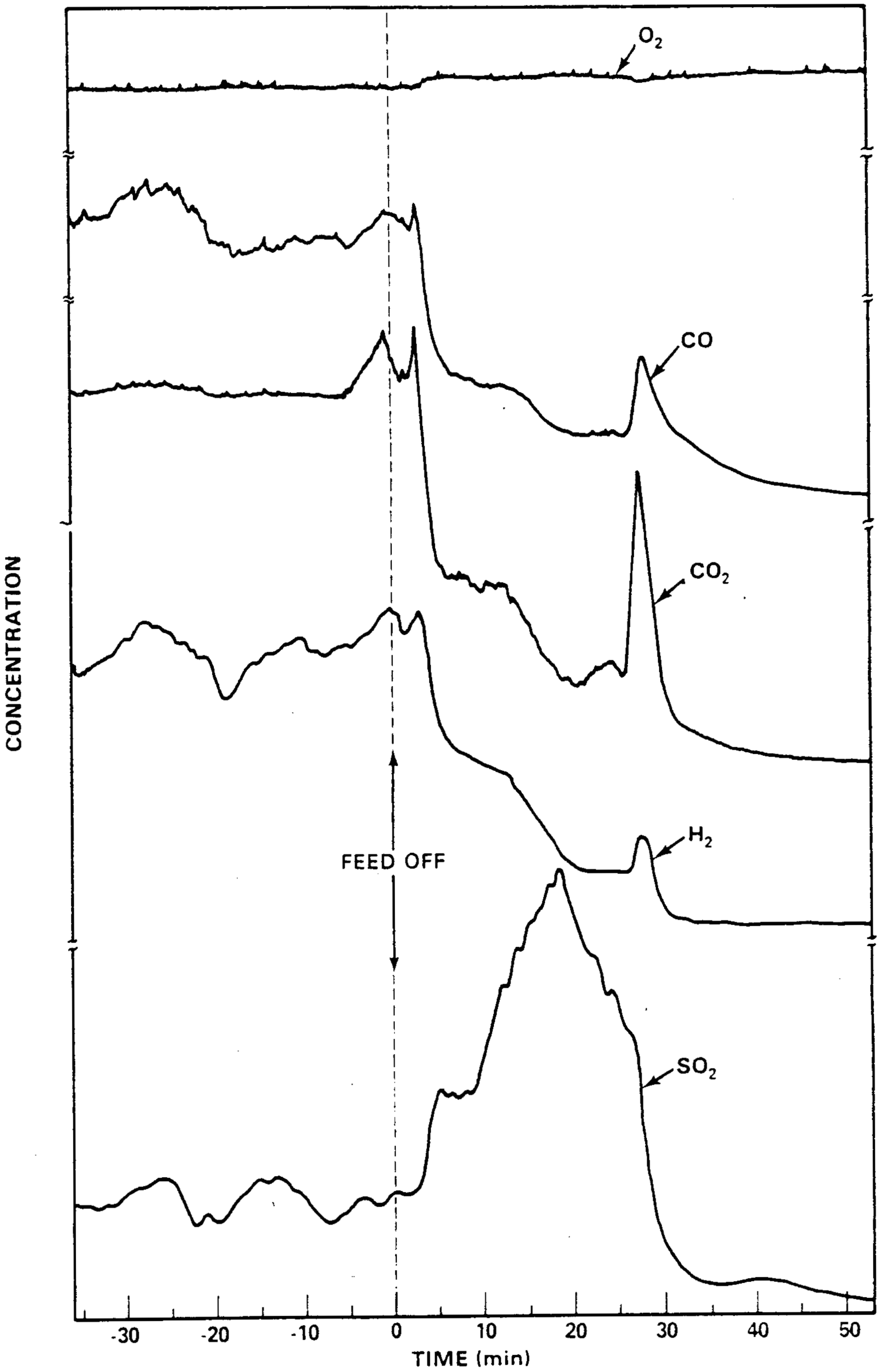

FIGURE 5. Melter Off-Gas Compositional Behavior Associated With Feed Termination. The t = 30 min Compositional Spike is due to the Injection of a Small Quantity of Liquid Feed

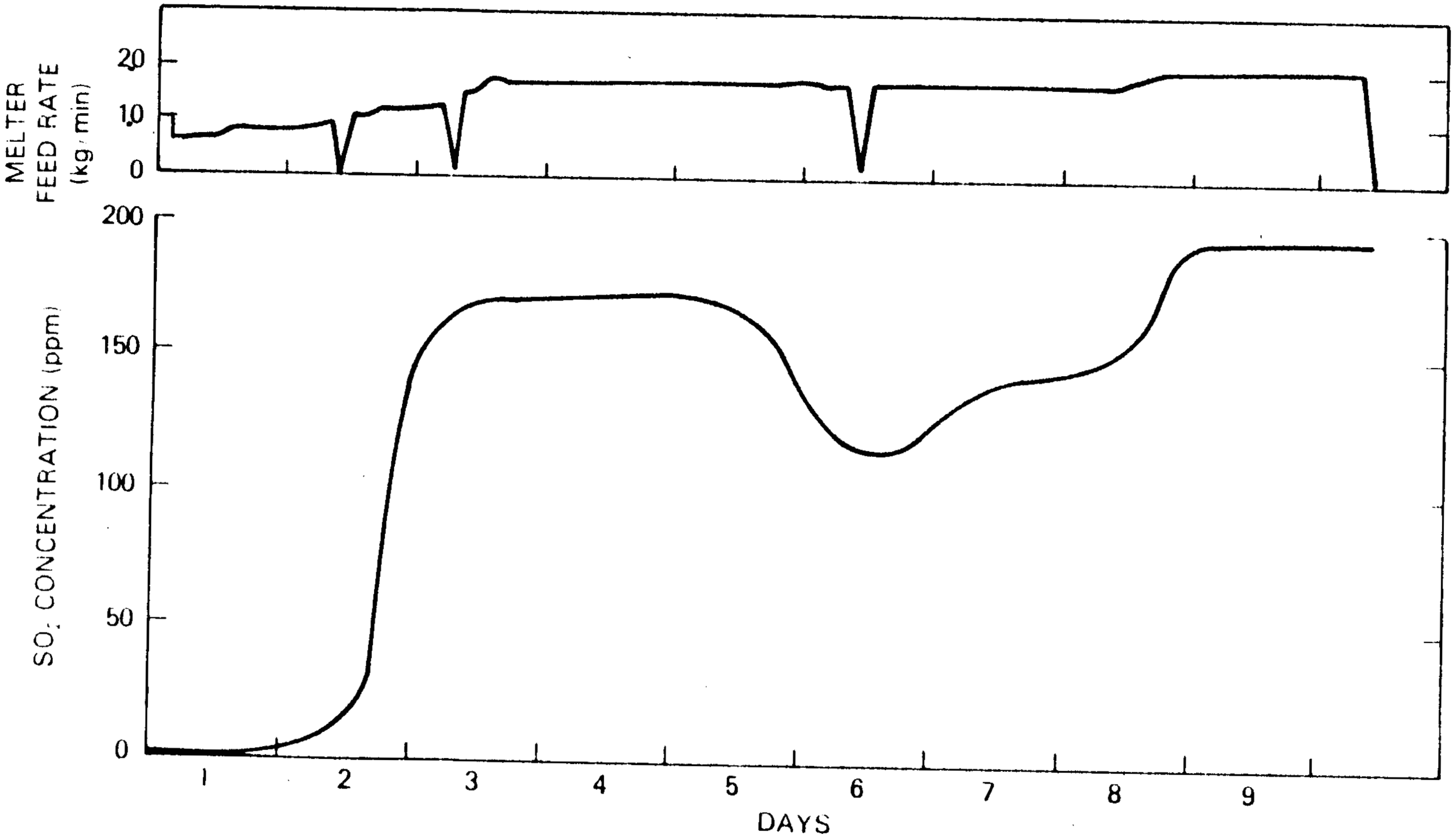

FIGURE 6. Melter SO_2 Emission Characteristics Accompanying a ~240-h Test

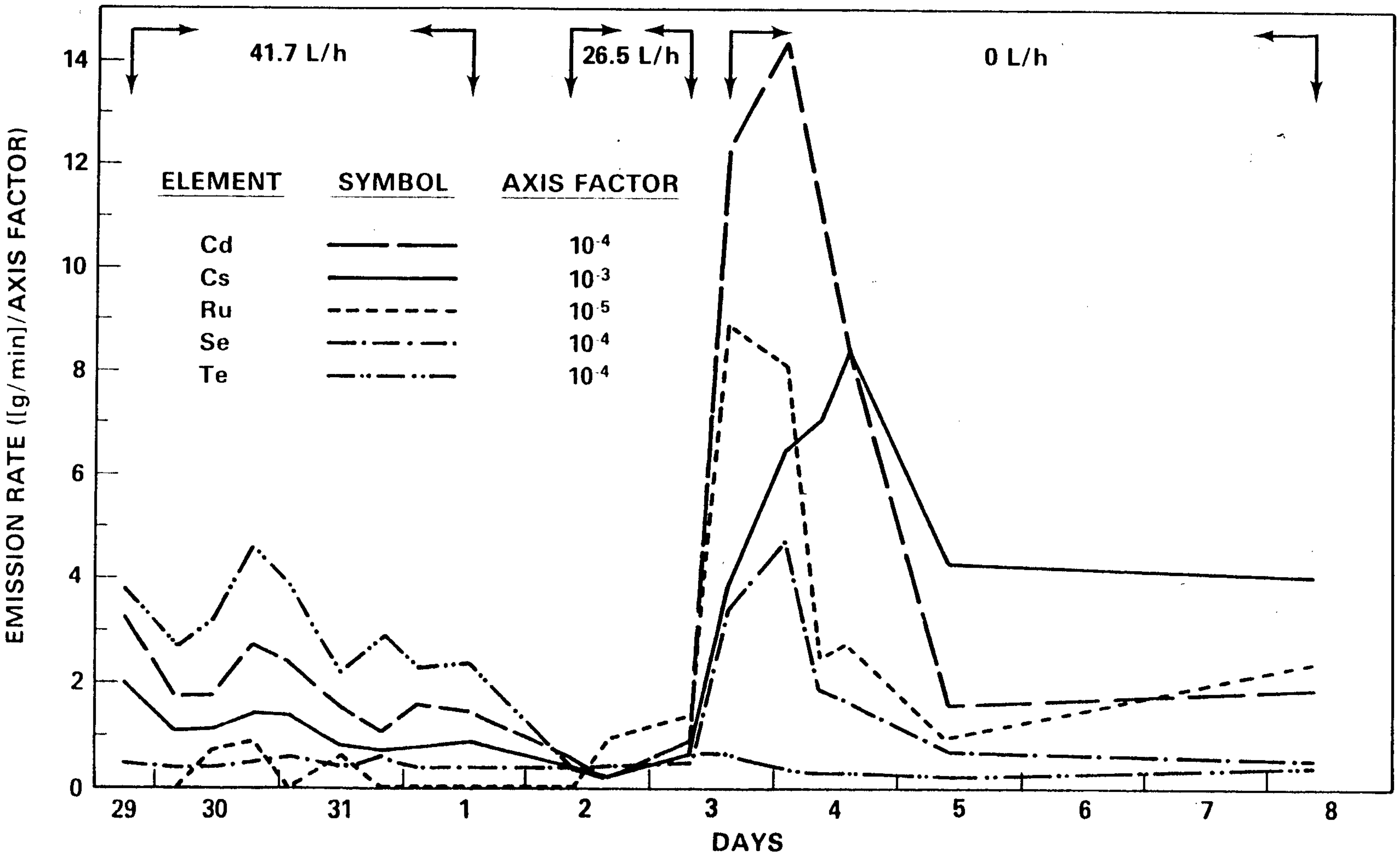

FIGURE 7. Melter Idling Emission Rates of Semivolatile Elements

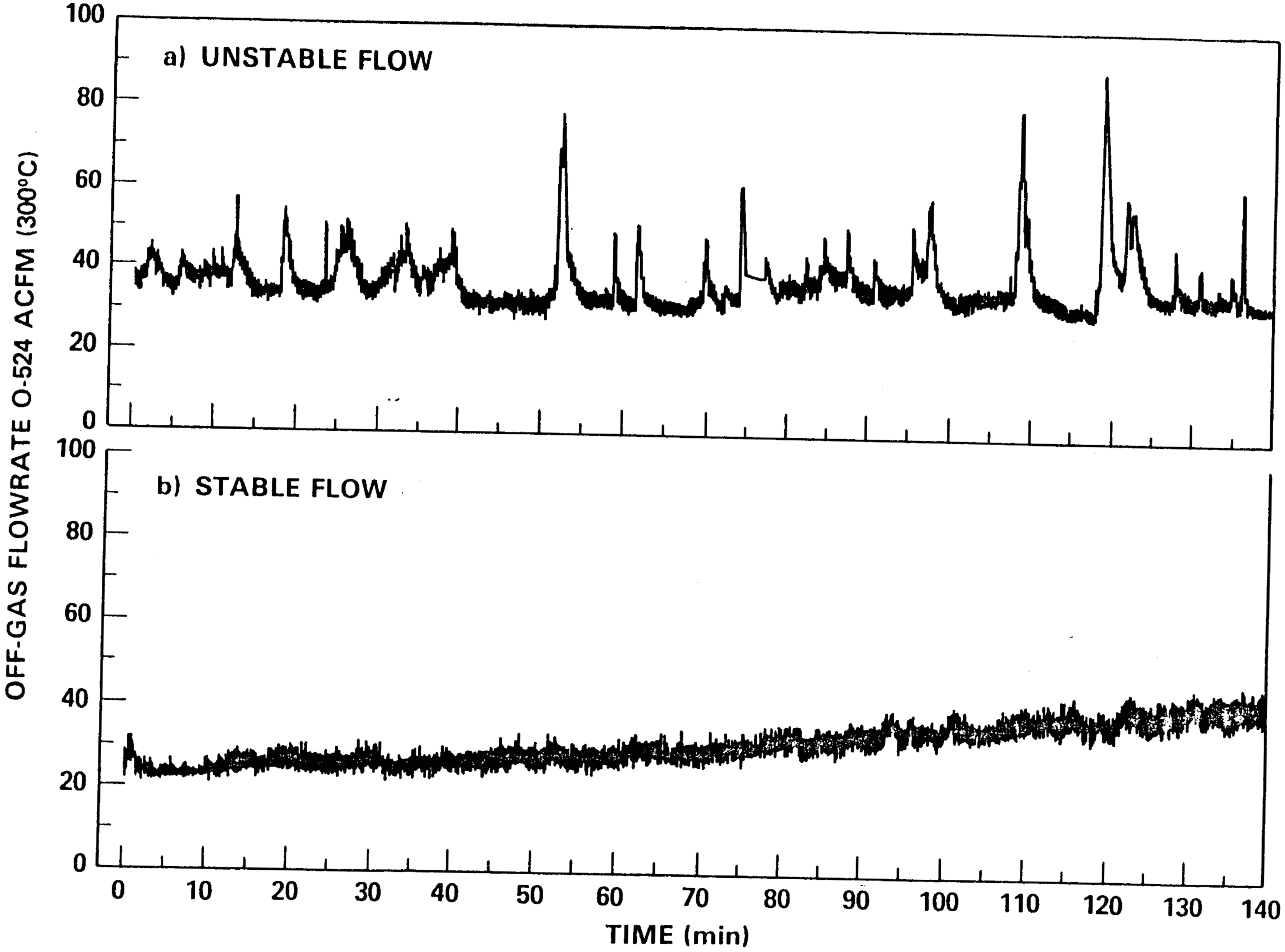

FIGURE 8. Typical Off-Gas Flow Rate Behavioral Patterns Associated with Liquid-Fed Melters